1-1-2015

First Principles Calculations of Doped Mnbi Compounds

Sultana Abdullah Ababtin

First principles calculations of doped MnBi compounds

By

Sultana Abdullah Ababtin

A Thesis
Submitted to the Faculty of
Mississippi State University
in Partial Fulfillment of the Requirements
for the Degree of Master of Science
in Physics
in the Department of Physics and Astronomy

Mississippi State, Mississippi

May 2015

First principles calculations of doped MnBi compounds

By

Sultana Abdullah Ababtin

Approved:

_____

Seong- Gon Kim
(Major Professor)

_____

James A. Dunne
(Committee Member)

_____

R. Torsten Clay
(Committee Member)

_____

R. Gregory Dunaway
Professor and Dean
College of Arts & Sciences

Name: Sultana Abdullah Ababtin

Date of Degree: May 9, 2015

Institution: Mississippi State University

Major Field: Physics

Major Professor: Seong- Gon Kim

Title of Study: First principles calculations of doped MnBi compounds

Pages in Study: 27

Candidate for Degree of Master of Science

We investigate the effect of the substitution of Ni, Ti and Co in MnBi using first principles calculations based on density functional theory (DFT) within the generalized gradient approximation (GGA). We also performed total energy calculations to compare different structures to determine the ground state structures and investigate their magnetic properties. Our calculation shows that the substitution of Ni, Co and Ti lowers the total magnetization of MnBi. We also found that the stable structure of Ni and Ti substitute is to replace Mn atoms in their regular site while the substitute Co is most stable when Co occupies the interstitial site of MnBi unit cell.

Key Words: Density Functional Theory, MnBi, Magnetic properties.

ACKNOWLEDGEMENTS

I would not be the person who I am today without the help of many people. First of all, I am thankful to King Saud University for this grant to pursue my graduate studies. Many thanks to Mississippi State University and High Performance Computing Collaboratory HPCC for all the helps they provided throughout the way. I thank my advisor, Dr. Seong-Gon Kim for his continuous support, as well as the committee members, Dr.R. Torsten Clay, and Dr. James A. Dunne. Special thanks go to Professor David Monts for all the helps he has provided. I would like also to thank my research group, Dr. Sungho Kim, Chandani, and Vivek .I do not forget to thank my parents, family, friends, classmates and co-workers for their help and support.

TABLE OF CONTENTS

LIST OF TABLES

LIST OF FIGURES

CHAPTER I

INTRODUCTION

Computational science has opened a window of knowledge that is hard to be reached otherwise. In the recent years, it has grown widely to examine various natural phenomena and get the same results of real experiments. Yet, computational experiments save effort, time and money. One of the applications for computational science is studying materials properties. Material properties are mainly determined by the interactions between the electrons in the outer shells of the atoms, called the valance electrons. Therefore, the materials behavior can be understood and predicted by using quantum mechanics in the electronic scale. Solving Schrödinger's equation,$H\Psi = E\Psi$, is sufficient to predict the behavior of the constituents of materials, such as electrons and ions, where H is the Hamiltonian operator, E is the energy of the system, and Ψ is the wave function. However, this can be done only for a small system such as the hydrogen atom. It is impossible for any practical systems that are made up of large number of electrons and ions. Fortunately, it is still possible to obtain solutions to Schrödinger's equation in this case owing to the advances in algorithmic and fast computers. These methods are called first principles calculations because they are parameter-free and they require nothing more than the atom's type and location. We apply first principles calculations based on Density Functional Theory (DFT) [CMP15] in substituting Ni, Co

and Ti in MnBi to observe the effect on magnetic properties such as total magnetization of the substituted MnBi.

CHAPTER II

DENSITY FUNCTIONAL THEORY

2.1 Introduction

With the advancement in technology, computer programs are used to analyze the physical systems in the electronic scale. These are known as the computational methods. Density functional theory (DFT) is a modelling method widely used in different sciences to determine the electronic structure in atoms, molecules and condensed phases. Although it is an approximate method for many electron systems, it is one of the most reliable methods used in quantum chemistry today. The analysis is based on equations that include the exchange and correlation functional that states that the energy of the molecule is a dependent on electron density [CMP15]. Electron density is in turn dependent on the position of the electrons. There are several commonly used exchange-correlation functionals including the local density approximation (LDA) [FIO03] and generalized gradient approximation (GGA) [FIO03].

2.2 Born-Oppenheimer Approximation

It is a method used in density functional theory to describe the interactions within atoms and molecules. It refers to the assumption that the motion of an electron and that of a nucleus in a molecule are separable, creating a molecular wave function, which is a

function of the position of the electron and that of the nuclei. It consequently follows the expression:

$$\Psi_{molecule}(\vec{r_i}, \vec{R_j}) = \psi_{\text{electrons}}(\vec{r_i}, \vec{R_j})\psi_{\text{nuclei}}(\vec{R_j}) \quad (2.1)$$

where $\vec{r_i}$ is the position of the electron, while $\vec{R_j}$ is the position of the nucleus. In order for this approximation to hold, there are two basic assumptions involved. The first assumption is that; wavelength of an electron is determined by the position of the nuclei and not by the velocity of the individual molecules. This can be taken to assume that the motion of a nucleus is slow compared to that of an electron, to the extent that the former is considered static. The second assumption is that the motion of a nucleus, which includes vibration or rotation, can be reduced to a potential energy term in the electronic problem.

However, the forces on both electrons and nuclei caused by electric charge are deemed to be of the same order of magnitude and hence the changes which occur in their momenta due to these forces must be the same. Moreover, because its mass is much greater than the mass of electrons, the nuclei have much smaller velocities. On the typical time scale of nuclear motion, the electrons will rapidly relax to the instantaneous ground-state configuration such that in solving the time independent Schrodinger equation from the Hamiltonian equation. The assumption will be that the nuclei are stationary and therefore the electronic ground-state is first calculated and later calculate the energy of the system in order to solve for the nuclear motion. The Schrödinger equation and Hamiltonian operator are:

$$\Psi(R_1 .. R_j, r_1 .. r_i) = E\Psi(R_1 .. R_j, r_1 .. r_i) \tag{2.2}$$

$$\widehat{H} = -\sum_{i=1}^{M} \frac{h^2}{2m_{z_i}} \nabla_{R_j}^2 - \sum_{i=1}^{M} \frac{h^2}{2m_e} \nabla_{r_i}^2 + \frac{1}{4\pi\epsilon_0} \sum_{i=1}^{M} \sum_{j>i}^{M} \frac{Z_j Z_i e^2}{|R_i - R_j|} - \frac{1}{4\pi\epsilon_0} \sum_{i=1}^{N} \sum_{j=1}^{M} \frac{Z_j e^2}{|r_i - R_j|} + \frac{1}{4\pi\epsilon_0} \sum_{i=1}^{N} \sum_{j>i}^{N} \frac{e^2}{|r_i - r_j|} \tag{2.3}$$

where m_e is the electron mass, Z_i is the atomic number of the i^{th} nucleus, m_{zi} is the mass of the i^{th} nucleus, $\hbar$ is Planck's constant divided by 2π, and ε_0 is the permittivity of vacuum.

It is known that the mass of nuclei is much more than the mass of the electron, and its speed is slower than the electron as well. It can be assumed that the nuclei have fixed position $R_i \ldots . R_M$. Therefore, the first term of Eq(2.3) will be small and the potential energy of nuclei-nuclei interaction in this context is constant, so we can reformulate it as V_{II}. The Hamiltonian operator will then become within the Born-Oppenheimer Approximation.

$$\widehat{H} = \nabla_{r_i}^2 + V_{II} - \frac{1}{4\pi\epsilon_0} \sum_{i=1}^{N} \sum_{j=1}^{M} \frac{Z_j e^2}{|r_i - R_j|} + \frac{1}{4\pi\epsilon_0} \sum_{i=1}^{N} \sum_{j>i}^{N} \frac{e^2}{|r_i - r_j|} \tag{2.4}$$

2.3 Hohenberg-Kohn Theorems

These theorems are used in DFT to determine the ground state properties of a system. The theorems follow the Born-Oppenheimer approximation where the Coulomb potential that arises from a nuclei is treated as a static external potential. The first theory

states that "The external potential ($V_{\text{ext}}(r)$), and hence the total energy, is a unique functional of the electron density n(r)." [GHO11].

The second theorem states that "The ground-state energy can be obtained variationally: the density that minimizes the total energy is the exact ground-state density." [GHO11].

The Hohenberg-Kohn theorems are popular due to their powerful nature, but they are still considered to have a weakness in that they cannot be used to determine the density of a system in practice, especially that in ground state. It is possibly misleading since it can alter the actual state of DFT, which they are supposed to be in support. This led to the development of the next equation, the Kohn-Sham equation to try and address the weakness.

2.4 Kohn-Sham Equation

In his endeavours, Kohn –Sham developed an approach to unravelling the interacting many-particle concern in Physics. The methodology set to substitute the conventional interacting many-particle approach. Kohn – Sham's technique entailed an auxiliary system that relied on independent particles, also referred to as *Non-Interacting*.

Supposedly, the ground state particle density of the selected non-interacting many-particle approach equates to the ground state density of the initial interacting many-particle approach. Kohn – Sham ansatz articulates a range of the numerically solved single-particle equations for the non-interacting technique. Indeed, the estimates to the *exchange-correlation energy functional* determine the accuracy of the solution, which

integrate many-particle interaction conditions (Su, Jiang, Chen & Wu, 2014). Thus, to achieve the kinetic energy of the Non-Interacting many-particle technique;

$$T[n(\boldsymbol{r})] = -\frac{\hbar^2}{2m}\sum_i^n \langle\psi_i|\Delta^2|\psi_i\rangle \tag{2.5}$$

where ψ_i Represents Kohn-Sham orbitals.

The total particle density of the auxiliary technique emanates from the summative of occupied states.

$$n(\boldsymbol{r}) = \sum_{occ}\psi_i^*(\boldsymbol{r})\psi_i(\boldsymbol{r}) \tag{2.6}$$

The technique depicts derivations to the total energy of the system as;

$$E[n(\boldsymbol{r})] = T_s[n(\boldsymbol{r})] + V_{ext}(r)n(\boldsymbol{r})d\boldsymbol{r} + \frac{1}{2}\int\frac{n(r)n(r\prime)}{|r-r\prime|}\,d\boldsymbol{r}d\boldsymbol{r}' + E_{xc}[n(\boldsymbol{r})] \tag{2.7}$$

where $V_{ext}(r)$ Denotes the external potential (material's iconic potential), and $E_{xc}[n(\boldsymbol{r})]$ represents the exchange-correlation energy functional including the undefined interaction conditions of the estimated many-particle technique.

The following formulae emanates from keying in the minimization of total energy in regard to density through variational principle single-particle equations for the Khon-Sham auxiliary technique.

$$\left[-\frac{\hbar^2}{2m}\Delta^2 + V_{eff}\big(\boldsymbol{r}, n(\boldsymbol{r})\big)\right]\psi_i = \epsilon_i\psi_i \tag{2.8}$$

The above formulas represent the prominent Kohn-Sham equations. They have elicited a shit from the many-particle problem to a single particle moving in an efficient potential usually generated by other particles in the system.

$$V_{eff}(\boldsymbol{r}, n(\boldsymbol{r})) = V_{ext}(\boldsymbol{r}) + \int \frac{n(\boldsymbol{r}')}{|\boldsymbol{r}-\boldsymbol{r}'|} + \frac{E_{xc}}{n\ (\boldsymbol{r}')} \quad (2.9)$$

Kohn-Sham aimed at establishing the ground state particle density as provided for in the equations (2.6). Briefly, the technique by Kohn-Sham led to the alteration of the energy functional equation

$$E[n(\boldsymbol{r})] = T_s[n(\boldsymbol{r})] + V_{ext}(r)n(\boldsymbol{r})d\boldsymbol{r} + \frac{1}{2}\int \frac{n(r)n(r\prime)}{|r-r\prime|}\ d\boldsymbol{r}d\boldsymbol{r}' + E_{xc}[n(\boldsymbol{r})] \quad (2.10)$$

Thus, giving the range of self-consistently resolved differential equations. The applicability of this technique critically underlies the E_{xc} functional characterized by the absence of an analytical expression, hence the essentiality of estimations [SUP14][MAI10].

2.5 Local Density Approximation (LDA)

LDA may also go by the term Local Spin Density Approximation (LSDA). The approximations operate under an assumption that the local electron density determines the exchange-correlation energy through the following formula:

$$E_{xc}[n(r)] = \int n(r) \in_{xc} [n(r)]dr \quad (2.11)$$

The $E_{xc}[n(r)]$ represents the energy in each electron, and it relies on the density, $n(r)$ that is close to r. $E_{xc}[n(r)]$ is universal, meaning that the parameters might be similar to those of a homogenous electron gas. Going by the above assumption, then $E_{xc}[n(r)]$ entails an analytical concept (TAN12]. Ceperly and Alder calculated the correlation section by applying the Monte-Carlo methods.

2.6 Generalized gradient approximation (GGA)

GGA accommodates the density of the electron during the examination of the exchange-correlation energy, unlike LDA. The formula is as follows:

$$E_{xc}[n(r), \nabla n(r)] = \int n(r) \in_{xc} n(r), \nabla n(r)]dr \quad (2.12)$$

The GGA applies the parametric principles of Perdew-Wang and Perdew-Burke-Ernzerhof.

2.7 Pseudopotential

The external environment affects the valence electrons more than those closer to the atomic core. Based on the assumption that the core electrons are static, the pseudopotential approach enacts a new force on the core electrons effect and coulomb potential. The force leads to wave-like forces on the valence electrons [TAN12]. The force usually has a smoother effect, thus leading to a lower number of the plane waves representing the electrons. In effect, the overall energy converges at a faster rate. The full wave and the pseudo wave functions resemble each other at the area behind the cutoff radius. The resemblance leads to the pseudo and electron wave functions producing charges of the same densities. The introduction of the ultra-soft pseudopotentials do not affect the norm conservation situation, thus benefiting the radii of the softer wave functions and the smaller cutoff. The fact that there might exist a drawback in the pseudopotentials is due to the lack of linearity of the exchange-correlation in the DFT. Moreover, remedies to the non-linear structure are necessary in order to accurately describe the interactions of the valence-core in case of a significant effect in the overlap between the core and the valence electron [TAN12]. The projector-augmented wave

(PAW) by Blochl engages in the reconstruction of the density of an electron and also accommodates for linearity in the exchange correlations to avoid the remedies. In the research, I applied PAW-GGA.

2.8 Basis Set

When practically solving Kohn-Sham equations, one does so through regular iteration. The process is accomplished through expanding the orbitals of the basis function sets that are chosen accordingly. One of the basis sets that can be adopted is one of plane-waves, which has three unique advantages. First, plane-waves ensure the basis-set convergence is controlled. Secondly, it enables one to use Hellmann-Feynman theorem, which enables the computation of all forces that act on atoms as well as evaluating the unit cell, before computing the stresses on that atom. Finally, it helps analyze a system and its time evolution, by opening up quantum molecular dynamic simulations from the beginning [AMI10].

2.9 Hybrid Density Functions

Hybrid functions are used to determine the electronic properties of metals and other solids, this can therefore be used to determine and improve their performance. It also has been used in mechanics to determine the nonlinear oscillations in metallic objects. For example it can be used to improve the photoconductivity of solar energy applications for example in Cuprous Oxide. It has been realized that the photoconductivity of Cuprous Oxide (Cu_2O) is limited by its electron carrier minority. By determining the electronic structure and its density, a hybrid function can then be used to

predict a delocalized electron and a localized electron thus improving its photoconductivity [LSS13].

We used the Heyd-Scuseria-Ernzerhof (HSE) density functionals. They are favored because they are able to advance based upon the preciseness of semilocal functionals, especially for the gaps of semiconductor band. The form of HSE functional defines a two-dimensional space of DFT functionals, set by the fraction of Fock exchange, a,at zero electron separation and length scale, ω^{-1}, on which the short-range Fock exchange is computed [MOU12].

$$\mathrm{E_{xc}} = \mathrm{aE_x^{\mathit{HF},SR}}(\mu) + (1 + \mathrm{a})\,\mathrm{E_x^{PBE,SR}}(\mu) + \mathrm{E_x^{PBE,LR}} + \mathrm{E_c^{PBE}} \qquad (2.13)$$

CHAPTER III

SUBSTITUTION OF NI, CO AND TI IN MNBI

3.1 Introduction

In the recent years, much attention has been paid to the study of rare earth free permanent magnetic materials. Such scientific interest can be explained by search of substitutes for rare earth based magnets technologically important. As it is widely known, rare earth based magnets are rare and expensive. That is why, Mn-based intermetallic materials gain popularity in scientific community all over the world, mainly MnBi [KHA10] and MnAl [JIM12]. Due to their structural and magnetic properties MnBi and MnAl are strategically important compounds with permanent magnetic performance and crystallographic characteristics that can be used as innovative thermal writing means [SAH2000, YIN96]. In correspondence to synthesis temperature binary system of MnBi demonstrates three magnetic phases. While synthesizing MnBi at temperature below 355° C it goes through first order structural and magnetic transition to a paramagnetic high temperature phase [KOY07, YIN96]. When high temperature MnBi is quickly quenched a ferromagnetic quenched high temperature phase with Curie temperature of 167 °C is gained. Thus, satisfactory magnetic and magneto-optical properties of MnBi binary system are proved [SAH02].

Favorable hard magnetic properties characterize MnBi in its low temperature phase. It is worthy of attention that a coercive force of the low temperature

ferromagnetic phase (with coercivity value of 1.9 Tesla) rises at temperature 277°C [SAH02]. Taking into consideration of discussed properties, the low-temperature ferromagnetic phase MnBi is a great potential candidate for permanent magnetic material. The method of preparation and heat treatment determine MnBi crystal structure and its magnetic properties. Scientists marked MnBi simultaneous phase formation of several phases [XUG89]. It is difficult to get a separate phase MnBi with a help of traditional methods. Such a phenomenon takes place because of immediate formation of Mn and Bi precipitates, in terms of necessary MnBi matrix. Creation of separate phase MnBi in vast quantities is still difficult because of Mn segregation at temperature 446°C [GUO92].

A Great amount of research has been conducted in order to synthesize separate phase MnBi [PIR79, ROB56, and YOS99]. Such researchers as Yang [YAN02] and Zhang [ZHA11] successfully obtained MnBi permanent magnets of different quality through complicated synthesis routs. Some scientists gained 90% wt. low temperature ferromagnetic phase MnBi magnets by applying magnetic separation and other techniques [YAN02]. Also there were attempts to produce the MnBi magnet by quick quenching, followed by thermic treatment [GUO92]. In such a way scientists gained more than 95% wt. MnBi ferromagnetic of low temperature phase [GUO92]. Some years ago MnBi permanent magnet with density of 93% was prepared with application of milled powders elements [ZHA11]. Nithya et al. while studying structural and magnetic properties of the MnBi intermetallic compound (synthesis conditions for MnBi compound – vacuum seal and 310^{o}C/48h quenched) revealed that magnetic moments of MnBi are extremely dependent on heat treating schedule [NIT13].

So, different factors influence magnetic properties of MnBi such as fractional presence of different phases, compositions and microstructure. Thus, in order to enhance magnetic properties of MnBi detailed structural and compositional investigations are necessary.

A proper substitution of a foreign atom in MnBi unit cell can be used to tune the properties of MnBi. We have performed first principles calculations using DFT to study Co, Ni and Ti substituted MnBi.

3.2 Computational Method

MnBi has a hexagonal NiAs crystal structure that belongs to $P6_3/mmc$ space group. Fig 3.1 shows a unit cell of MnBi used in the present work that contains four atoms of two formula units. Magnetism in MnBi arises from Mn atoms occupying 2a site while Bi occupies 2c site [SHR13]

Total energies and forces were calculated using DFT with projected augmented wave (PAW) potentials as implemented in The Vienna Ab initio Simulation Package (VASP). All calculation were spin polarized. A plane wave cutoff of 520 eV was used for pure MnBi and substituted MnBi. Reciprocal space was sampled with a $8 \times 8 \times 6$ Monkhorst-Pack mesh. Electron exchange and correlation was treated with GGA as parameterized by the Perdew-Burke-Ernzerhof (PBE) scheme. To describe MnBi and substituted MnBi system correctly, we used GGA+U as well as HSE methods.

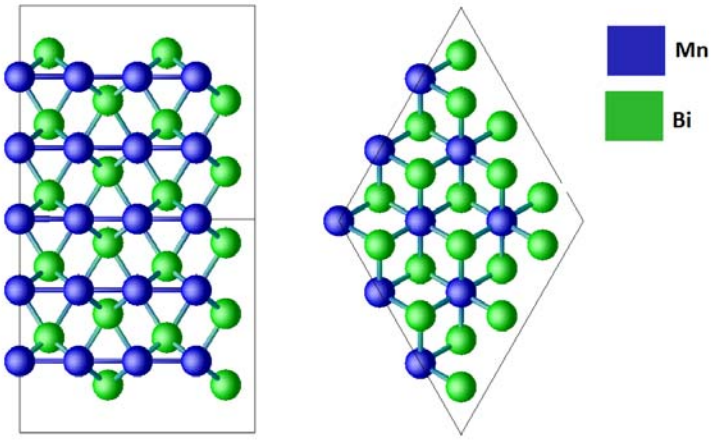

Figure 3.1 The Unit cell of MnBi in a hexagonal NiAs crystal structure

3.3 Results and discussion

3.3.1 Pure MnBi

We used DFT + U method to describe strongly correlated d-electrons of Mn atoms in MnBi. We performed a series of total energy calculations for different U_{eff} values. It has been noticed that the total magnetic moment of the unit cell increase as U_{eff} of Mn atom increases. To select the best U_{eff} value for Mn we performed a HSE calculation. Although HSE calculations are computationally much more demanding, it is considered to be more reliable than DFT+U calculations. HSE calculations estimated the total magnetic moment to be 8.153 μ_B. As shown in [Fig3.2] if we set U_{eff} to be around 5 eV we get around 8.153 μ_B. We therefore set U_{eff} to be 5 eV for all subsequent calculations for this work.

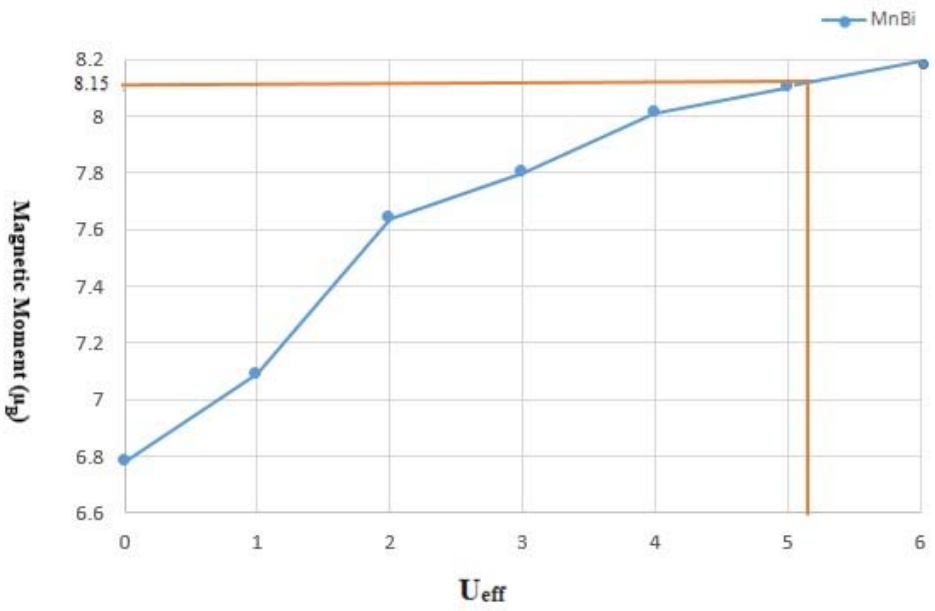

Figure 3.2 Calculated moment as a function of U_{eff}

We calculated lattice constants $a = 4.48$Å and $c = 6.058$Å while the experimental lattice constants of pure MnBi are $a = 4.256$Å and $c = 6.042$Å at 4.2 K [ROB56]. Table 3.1 shows the total energy of the MnBi unit cell and magnetization for U_{eff}=0.0 and 5.0 eV.

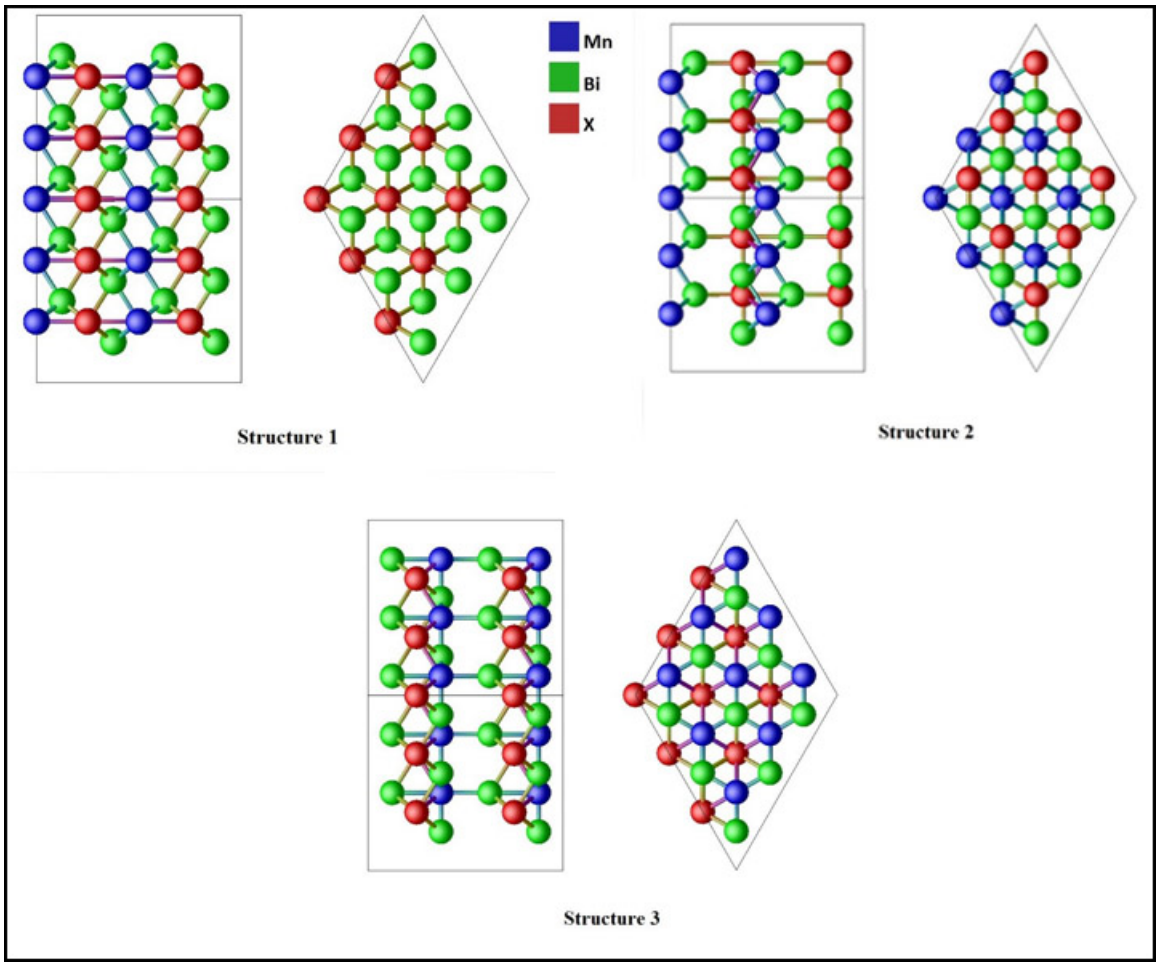

Figure 3.3 (i) Structure 1 X substituted in a regular lattice site of Mn.(ii) Structure**2** substituted in interstitial site with one of the lattice sites empty, and (iii) Structure3 disorganize structure by substituted in the regular lattice site of Mn and the second Mn occupies the interstitial site.

3.3.1.1 Ni substituted MnBi

In this case we added one Ni atom and removed one Mn atom from the unit cell of MnBi in Structure 1. Table 3.2 shows the effect of U_{eff} on the substitution energy and magnetization. For U_{eff} = 0 the substitution energy is negative which indicates that Ni substituted MnBi can be synthesized experimentally. However for other values of U_{eff} the substitution energy is a small positive number (< 1 eV). Considering the fact we have

not investigated the full phase space and we do not know U_{eff} of Mn and Ni which depends on neighboring atoms, a small positive value of substitution energy does not eliminates the possibility of formation of Ni substituted MnBi.

Table 3.1 One Ni atom has been substituted in MnBi unit cell.

Element	*U_{eff} (eV)*	*Energy (eV)*	*substitution Energy (eV)*	*Magnetic Moment (μ_B)*	*Magnetization $\mu_B/(\text{Å})^3$*
Mn_1Bi_2 Ni_1	0.0	-21.927	-0.369	4.1436	0.0474
	1.0	-19.541	0.072	4.671	0.0492
	2.0	-18.637	0.033	4.7149	0.0505
	3.0	-18.026	0.029	4.7354	0.0509
	4.0	-17.433	0.026	4.7661	0.0512
	5.0	*-16.861*	*0.022*	*4.9228*	*0.0527*

The value of U_{eff} has been varied to investigate its effect on E_{sub} and Magnetization

Next we investigate the possibility where substituted Ni atom does not go to the regular Mn site but forms Structure 2 or Structure 3. Table 3.3 compares the total energy of three cases. Here we have used HSE method which is considered to be a more accurate method without adjustable parameter U_{eff}. We see in the Table 3.3 that the energy of the unit cell in Structure 1 is the lowest energy. This indicates that the substituted atom takes a regular Mn site equally likely with ferromagnetic and antiferromagnetic Spin configuration.

Table 3.2 Comparison of Ni substituted MnBi in three different structures.

Element	*Case*	*Spin configuration*	*E_{tot} (eV)*	*Magnetic Moment (μ_B)*	*Magnetization $\mu_B/(\text{Å})^3$*
$Mn_1Bi_2Ni_1$	Structure (i)	FM	-29.0377	-5.1547	-0.0480
		AFM	-29.0378	-5.1554	-0.0480
	Structure (ii)	FM	-28.696	4.5196	0.0414
		AFM	-28.599	3.0634	0.0281
	Structure (iii)	FM	-27.720	5.0296	0.0461
		AFM	*-27.710*	*2.8418*	*0.0260*

FM and AFM indicate that Ni atoms have spins parallel and antiparallel to Mn atoms respectively.

3.3.1.2 Co substituted MnBi

In this case we substituted one Co atom in the MnBi unit cell. Table 3.4 show the effect of changing $U_{eff.}$. Similar to the previous case the substitution energy is only negative for the case $U_{eff} = 0$.

Table 3.5 shows comparison of total energy of the unit cell for different structures. Here we see the energy is lowest when Co atom sits in the interstitial site and its spin lies parallel to the spin of Mn atom.

Table 3.3 One Co atom has been substituted in MnBi unit cell.

Element	*U_{eff} (eV)*	*Energy (eV)*	*substitution Energy (eV)*	*Magnetic Moment (μ_B)*	*Magnetization $\mu_B/(\text{Å})^3$*
$Mn_1Bi_2Co_1$	0.0	-23.172	-0.066	4.2939	0.0507
	1.0	-20.189	0.4913	5.0002	0.0548
	2.0	-19.382	0.4779	5.2903	0.0570
	3.0	-18.734	0.3244	5.6226	0.0591
	4.0	-18.221	0.1772	5.7354	0.0603
	5.0	*-17.787*	*0.1086*	*5.7940*	*0.0594*

The value of U_{eff} has been varied to investigate its effect on E_{sub} and Magnetization

Table 3.4 Comparison of Co substituted MnBi in three different structures.

Element	*Case*	*Spin configuration*	*E_{tot} (eV)*	*Magnetic Moment (μ_B)*	*Magnetization $\mu_B/(\text{Å})^3$*
$Mn_1Bi_2Co_1$	Structure (i)	FM	-31.1693	2.1691	0.0202
		AFM	-31.1692	2.1706	0.0202
	Structure (ii)	FM	-31.189	5.6023	0.4757
		AFM	-30.954	1.8760	0.1593
	Structure (iii)	FM	-29.820	6.7316	0.5716
		AFM	*-29.887*	*2.6594*	*0.2258*

FM and AFM indicate that Ni atoms have spins parallel and antiparallel to Mn atoms respectively**.**

3.3.1.3 Ti Substituted MnBi

In this case we substituted one Ti atom in the MnBi unit cell. Table 3.6 shows the comparison of substitution energy and magnetization for different U_{eff} values.

We notice from the table that the substitution energy is negative in all values of U_{eff} except $U_{eff} = 3.0$ eV. Table 3.7 shows the comparison of three different structure. The total energy of the three different structures suggests that the first structure where Ti atom is substituted at a regular Mn lattice site is equally likely with ferromagnetic and antiferromagnetic spin configuration.

Table 3.5 One Co atom has been substituted in MnBi unit cell.

Element	*U_{eff} (eV)*	*Energy (eV)*	*substitution Energy (eV)*	*Magnetic Moment (μ_B)*	*Magnetization $\mu_B/(\text{Å})^3$*
$Mn_1Bi_2Co_1$	0.0	-23.172	-0.066	4.2939	0.0507
	1.0	-20.189	0.4913	5.0002	0.0548
	2.0	-19.382	0.4779	5.2903	0.0570
	3.0	-18.734	0.3244	5.6226	0.0591
	4.0	-18.221	0.1772	5.7354	0.0603
	5.0	*-17.787*	*0.1086*	*5.7940*	*0.0594*

The value of Ueff has been varied to investigate its effect on Esub and Magnetization

Table 3.6 Comparison of Co substituted MnBi in three different structures.

Element	*Case*	*Spin configuration*	*E_{tot} (eV)*	*Magnetic Moment (μ_B)*	*Magnetization $\mu_B/(\text{Å})^3$*
$Mn_1Bi_2Co_1$	Structure (i)	FM	-31.1693	2.1691	0.0202
		AFM	-31.1692	2.1706	0.0202
	Structure (ii)	FM	-31.189	5.6023	0.4757
		AFM	-30.954	1.8760	0.1593
	Structure (iii)	FM	-29.820	6.7316	0.5716
		AFM	*-29.887*	*2.6594*	*0.2258*

FM and AFM indicate that Ni atoms have spins parallel and antiparallel to Mn atoms respectively.

3.3.1.4 Ti Substituted MnBi

In this case we substituted one Ti atom in the MnBi unit cell. Table 3.6 shows the comparison of substitution energy and magnetization for different U_{eff} values.

We notice from the table that the substitution energy is negative in all values of U_{eff} except $U_{eff} = 3.0$ eV. Table 3.7 shows the comparison of three different structure. The total energy of the three different structures suggests that the first structure where Ti atom is substituted at a regular Mn lattice site is equally likely with ferromagnetic and antiferromagnetic spin configuration.

Table 3.7 One Ti atom has been substituted in MnBi unit cell.

Element	*U_{eff} (eV)*	*Energy (eV)*	*substitution Energy (eV)*	*Magnetic Moment (μ_B)*	*Magnetization $\mu_B/(\text{Å})^3$)*
$Mn_1Bi_2Ti_1$	0.0	-24.287	-0.522	3.9006	0.0412
	1.0	-21.409	-0.133122	5.0771	0.0491
	2.0	-20.587	-0.150681	3.8096	0.0362
	3.0	-17.523	2.075474	0.6707	0.0066
	4.0	-19.264	-0.313442	5.3303	0.0491
	5.0	*-18.832*	*-0.332984*	*-5.1992*	*-0.0457*

The value of Ueff has been varied to investigate its effect on Esub and Magnetization

Table 3.8 Comparison of Ti substituted MnBi in three different structures.

Element	*Case*	*Spin configuration*	*E_{tot} (eV)*	*Magnetic Moment (μ_B)*	*Magnetization $\mu_B/(\text{Å})^3$)*
$Mn_1Bi_2Ti_1$	Structure (i)	FM	-32.169	3.5924	0.0334
		AFM	-32.168	3.5925	0.0334
	Structure (ii)	FM	-30.525	5.1020	0.0467
		AFM	-30.574	2.6975	0.0247
	Structure (iii)	FM	-28.9741	1.2907	0.0118
		AFM	-28.9742	1.2909	0.0118

FM and AFM indicate that Ni atoms have spins parallel and antiparallel to Mn atoms respectively.

3.4 Conclusion

We investigated the substitution of Ni, Co and Ti atom in MnBi. DFT with GGA functional indicate that substitution energies of these elements are negative. However, DFT+U method calculated the substitution energies to be small positive number for substituted Ni and Co but it is negative for substituted Ti except when $U_{eff} = 3$. We also compared the total energies of three different structures using HSE method so there is no

U_{eff}. Our results show that Ni and Ti atoms go to the regular Mn lattice site in MnBi unit cell equally likely with ferromagnetic and antiferromagnetic spin configuration.

A Co atom has the lowest energy when Co occupies interstitial lattice site of MnBi unit cell and spins parallel to Mn atom.

REFERENCES

[ADA52] Adams, E., Hubbard, W. M., & Syeles, A. M. (1952). A New Permanent Magnet from Powdered Manganese Bismuthide. Journal of Applied Physics, 23(11), 1207.

[AMI10] Moitra, A. (2010). Atomistic simulations to study magnetic, mechanical, and thermal properties of materials using density functional theory and semi-empirical methods. [electronic resource]. Mississippi State : Mississippi State University, 2010.

[BUR05] Burke, K., Werschnik, J. & Gross, E.K. (2005). Time-dependent density functional theory: Past, present, and future. *The Journal of Chemical Physics*123 (6): 062206

[CHE74] Chen, T. (1974). Contribution to the equilibrium phase diagram of the Mn-Bi system near MnBi. Journal Of Applied Physics, 45(5), 2358-2360.

[CHR13] Christopher, N., Mishra, S, Singh, N., Singh, S., Gahtori, B., Dhar, A., & Awana, V. (2013). Appreciable magnetic moment and energy density in single-step normal route synthesized MnBi. Journal Of Superconductivity And Novel Magnetism, 26(11), 3161-3165.

[CMP15] Computational Materials Physics » VASP. (n.d.). Retrieved March 12, 2015, from https://cmp.univie.ac.at/research/vasp/.

[COE11] Corey, J. (a.n.d). Hard Magnetic Materials: A Perspective. Ieee Transactions On Magnetics, 47(12), 4671-4681. Coey, J.M.D., (2012). Permanent magnets: plugging the gap. *Scripta Materialia, 67*, 524.

[FIO03] Fiolhais, C., Nogueira, F. & Marques, M. (2003). *A Primer in Density Functional Theory*. Springer. Materials Today, 659.

[GAO13] Gao, T. R., Wu, Y. Q., Fackler, S.,Kierzewski, I., Zhang Y. et al., (2013).Combinatorial exploration of rare-earth-free permanent magnets: Magnetic and microstructural properties of Fe-Co-W thin films. *Appl. Phys. Lett. 102*, 022419.

[GHO11]Ghouri, M. (2011). Methodology. In *Computational study on novel carbon-based lithium materials for hydrogen*. S.l.: Proquest, Umi Dissertatio.

[GUO91] Guo, X., Altounian, Z., & Ström-Olsen, J. O. (1991). Formation of MnBi ferromagnetic phases through crystallization of the amorphous phase. Journal Of Applied Physics, 69(8), 6067.

[GUO92] Guo, X., Chen, X., Altounian, Z., & Ström-Olsen, J. (1992). Magnetic properties of MnBi prepared by rapid solidification. Physical Review B, 46(22), 14578-14582.

[HEH03] Hehre, W.J. (2003). *A Guide to Molecular Mechanics and Quantum Chemical Calculations*. Irvine, California: Wavefunction, Inc

[JIM12] Jime´nez-Villacorta, F., Marion, J. L.,Sepehrifar, T., Daniil, M., Willard, M. A.,and Lewis, L. H., (2012). Exchange anisotropy in the nanostructured MnAl system. *Appl. Phy. Lett. 100*, 112408.

[KHA10] Kharel, P., Skomski, R., Kirby, R. D., & Sellmyer, D. J. (2010). Structural, magnetic and magneto-transport properties of Pt-alloyed MnBi thin films. Journal Of Applied Physics, 107(9), 09E303-1-09E303-3.

[KHA10] Kharel, P., Skomski, R., Kirby, R. D., and Sellmyer, D. J., (2010). Structural, magnetic and magneto-transport properties of Pt-alloyed MnBi thin films. *J. Appl. Phys. 107*, 09E303.

[KHA12] Kharel, P., Li, X. Z., Shah, V. R., Al-Aqtash, N., Tarawneh, K., Sabirianov, R. F., & ... Sellmyer, D. J. (2012). Structural, magnetic, and electron transport properties of MnBi:Fe thin films. Journal Of Applied Physics, 111(7), 07E326-07E326-3.

[KOY07]Koyama, K., Onogi Tetsuya, Mitsui Yoshifuru, Nakamori Yuko, Shin-ichiOrim and Kazuo Watanabe, (2007). Magnetic phase transition of MnBi under high magnetic fields and high temperature. *Materials Transactions, 48(9)*, 2414.

[KRA12] Kramer, M. J., McCallum, R.W.,Anderson, I.A. and Constantinides, S.,(2012). Prospects for non-rare earth permanent magnets for traction motors and generators JOM. *J. Min. Met.Mater. Soc. 64*, 752.

[LEB14] Lebègue, S. (2014). Introduction to Graphene-Based Nanomaterials: From Electronic Structure to Quantum Transport. By Luis E. F. Foa Torres, Stephan Roche and Jean-Christophe Charlier. Cambridge University Press, 2014. Pp. 320.

[LEP12] Lepley, N., & Holzwarth, N. (2012). Computer modeling of crystalline electrolytes: Lithium thiophosphates and phosphates. Journal of the Electrochemical Society, 159(5), A538-A547.

[LIY13] *Liyanage, Laalitha S. I.* (2013). Investigation of structure-property relationships in materials using Ab-initio and Semi-empirical methods. *ProQuest Dissertations and Theses; Thesis (Ph.D.)--Mississippi State University; Source: Dissertation Abstracts International*, Volume: 74-08(E), Section: B.; 93 p

[LSS13] Isseroff, L., & Carter, E. (2013). Electronic structure of pure and doped cuprous oxide with copper vacancies: Suppression of trap states. Chemistry Of Materials, 25(3), 253-265.

[MOI10] Moitra, A. (2010). Atomistic simulations to study magnetic, mechanical, and thermal properties of materials using density functional theory and semi-empirical methods.

[MOR06] Moran, D., Simmonett, A.C., Leach, F.E., Allen, W.D., Schleyer, P.R. & Schaefer, H.F. (2006). Popular Theoretical Methods Predict Benzene and Arenes To Be Nonplanar *Journal of the American Chemical Society*128 (29): 9342–3

[MOU12] Moussa, J. E., Schultz, P. A., & Chelikowsky, J. R. (2012). Analysis of the Heyd-Scuseria-Ernzerhof density functional parameter space. Journal Of Chemical Physics, 136(20), 204117

[NIT13] Nithya, R.Ch., Singh. N., Singh, Sh. K., Gahtori, B., Mishra, S.K., Dhar, A., Awana, V.P.S. (2013). Appreciable magnetic moment and energy density in single step normal route synthesized MnBi. *J Supercond Nov Magn. 26*, 3161-3165.

[PAI06] Paier, J., Marsman, M., Hummer, K., Kresse, G., Gerber, I. C., & Ángyán, J. G. (2006). Screened hybrid density functionals applied to solids. *Journal of Chemical Physics*, 124(15), 154709.

[PAR94] Parr, R.G. & Yang, W. (1994). *Density-Functional Theory of Atoms and Molecules*. Oxford: Oxford University Press

[PIC02] Picozzi, S., Continenza, A., & Freeman, A. (2002). Co2MnX (X=Si, Ge, Sn) Heusler compounds: An ab initio study of their structural, electronic, and magnetic properties at zero and elevated pressure. Physical Review B - Condensed Matter And Materials Physics, 66(9), 944211-944219.

[PIR79] Pirich, R. G., and Larson, D. J., (1979). Magnetic and metallurgical properties of directionally solidified eutectic Bi/MnBi composites: the effects of annealing. *J. Appl. Phys. 50*, 2425.

[RAM13] Rama Rao, N. V., Gabay, A. M. and Hadjipanayis, G. C., (2013). Anisotropic fully dense MnBi permanent magnet with high energy product and high coercivity at elevated temperatures. *J. Phys. D: Appl. Phys. 46, 062001.*

[REI03] Reis, C.L., Pacheco, J. M. & Martins, J.L. (2003), First-principles norm-conserving pseudopotential with explicit incorporation of semicore states", *Physical Review B(American Physical Society)*68 (15): 155111

[ROB56] Roberts, B. (1956). Neutron diffraction study of the structures and magnetic properties of manganese bismuthide. Physical Review, 104(3), 607-616.

[ROB56] Roberts, B. W., (1956). Neutron diffraction study of the structures and magnetic properties of manganese bismuthide. *Phys. Rev. 104*, 607.

[SAH02] Saha, S., Obermyer, R. T., Zande, B. J., Chandhok, V. K., Simizu, S., Sankar, S. G. and Horton, J. A., (2002).Magnetic properties of the low-temperature phase of MnBi. *J. Appl. Phys. 91 (10)*, 8525.

[SAH2000] Saha, S., Huang, M. Q., Thong, C. J., Zande, B. J., Chandhok, V. K., Simizu, S.,Obermyer, R. T. and Sankar, S. G., (2000).Magnetic properties of MnBi1−xRx (R=rare earth) systems. *J. Appl. Phys. 87*, 6040.

[SEG02] Segall, M.D. & Lindan, P.J (2002). First-principles simulation: ideas, illustrations and the CASTEP code. *Journal of Physics: Condensed Matter*14 (11): 271

[SHO09] Sholl, D. S., & Steckel, J. A. (2009). Density functional theory : a practical introduction. Hoboken, N.J. : Wiley, c2009.pag 27,218-219,227-229

[TAN12] Tan, J., Li, Y., & Ji, G. (2012). Elastic constants and bulk modulus of semiconductors Performance of plane-wave pseudopotential and local-density-approximation density functional theory. *Computational Materials Science*, *58*, 243-247.

[XUG89] Xu, G. S., Lakshmi, C. S., Smith, R. W., (1989). MnBi phases in melt-spun Bi-Mn alloys. *Journal of Material Science Letters 8*, 1113.

[YAN01] Yang, J. B., Kamaraju, K., Yelon, W. B., James, W. J., Cai Q., and Bollero, A.,(2001). Magnetic properties of the MnBi intermetallic compound. *Appl. Phys. Lett.79*, 1846.

[YAN02] Yang, J. B., Yelon, W. B., James, W. J., Cai, Q., Roy, S., and Ali, N., (2002).Structure and magnetic properties of the MnBi low temperature phase. *J. Appl. Phys. 91*, 7866.

[YAN11] Yang, J. B., Yang, Y. B., Chen, X. G., Ma, X. B., Han, J. Z., Yang, Y. C., Guo, S., Yan, A. R., Huang, Q. Z., Wu, M. M.,and Chen, D. F., (2011). Anisotropic nanocrystalline MnBi with high coercivity at high temperature. *Appl. Phy. Lett. 99*, 082505.

[YIN96] Yin, F., Nanju, G., (1996). Sintering formation of low temperature phase MnBi and its disordering in mechanical milling. *J. Mater., Sci. Technol. 335*, 12.

[YOS99] Yoshida, H., Shima, T., Takahashi, T., and Fujimori, H., (1999). Preparation of highly pure MnBi intermetallic compounds by arc-melting. *Mater. Trans. 40 (5)*, 455.

[ZHA11] Zhang, D. T., Cao, S., Yue, M., Liu, W. Q., Zhang, J. X., Qiang, Y., (2011). Preparation and magnetic properties of bulk nanostructured PrCo5 permanent magnets with strong magnetic anisotropy. *J. Appl. Phys. 109 (7)*, 07A722.

[ZHA12] Zhang, X., Y. Wang, and Y. Ma. 2012. "High pressure structures of "111" type iron-based superconductors predicted from first-principles." *Physical Chemistry Chemical Physics* 14, no. 43: 15029-15035. *Scopus*®, EBSCO*host* (accessed March 14, 2015).